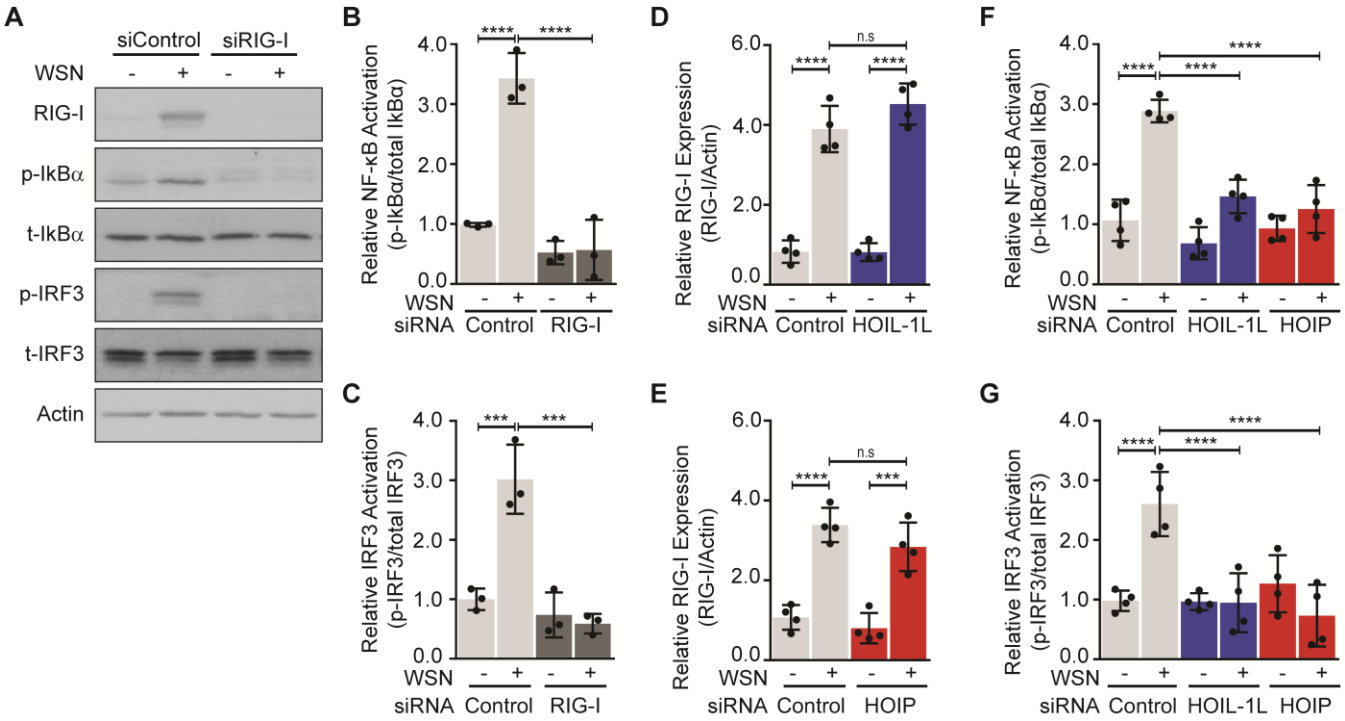

Supplemental Figure 1. LUBAC activates NF-κB and IRF downstream of RIG-I during IAV infection. (A) A549 cells were infected with WSN (1 MOI, 16 h) after transfection with a non-targeting siRNA (siControl) or siRNA against RIG-I. Representative immunoblot of NF-kB activation (p-IkBα/total IkBα) and IRF3 activation (p-IRF3/total IRF3) are shown **(B-C)** Bar graphs showing the quantification of **(B)** NF-κB and **(C)** IRF3 activation from **A** (n=3) **(D-E)** Bar graphs showing the quantification of RIG-I activation in the presence and absence of siRNA against **(D)** HOIL-1L or **(E)** HOIP from Figure 1A-B respectively (n=4). **(F-G)** Bar graphs showing the quantification of **(F)** NF-κB 1C and **(G)** IRF3 activation from Figure 1D-E respectively (n=4). Mean ± s.d. overlaid with individual data points representing replicates are depicted, **P* < 0.05, ***P* < 0.01, ****P* < 0.005, *****P* < 0.0001 (one-way ANOVA followed by Bonferroni post-hoc test).

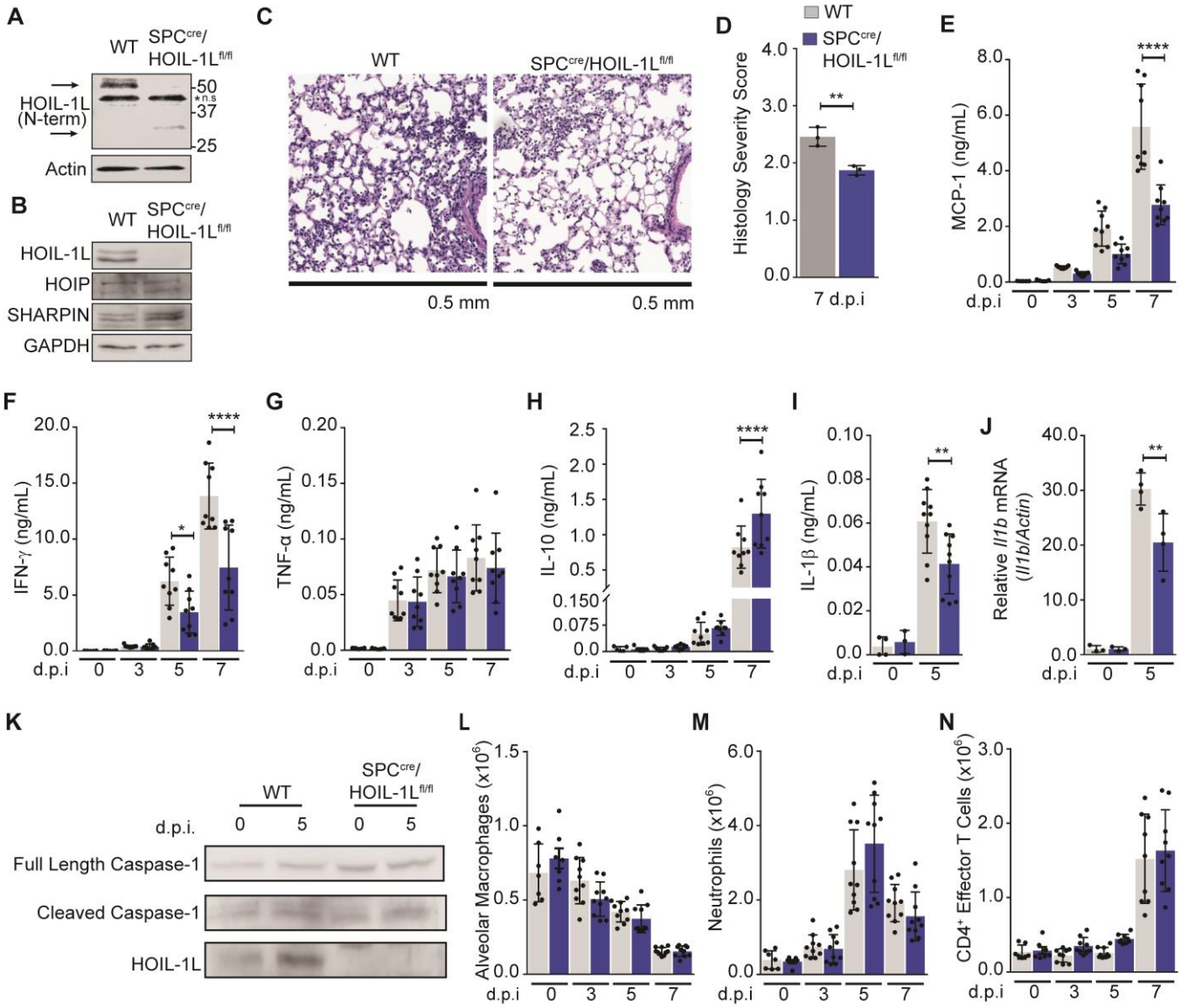

Supplemental Figure 2. Loss of HOIL-1L in the alveolar epithelium decreases inflammation during IAV infection in mice. WT and SPC^{cre}/HOIL-1L$^{fl/fl}$ mice were i.t. infected with a lethal dose of WSN **(A-B)** Representative immunoblot showing HOIL-1L, HOIP and SHARPIN expression in WT and SPC^{cre}/HOIL-1L$^{fl/fl}$ AT2 cells, n.s denotes non-specific band (n=3). **(C)** Brightfield images of lung sections from WT and SPC^{cre}/HOIL-1L$^{fl/fl}$ mice at 7 d.p.i. stained with H&E, and **(D)** quantified for severity of lung injury as defined in Methods (Scale bar, 0.5 mm.) **(E-H**) BALF cytokine levels were analyzed by ELISA at 0 (n=5) and 3, 5, 7 d.p.i. (n=9) **(E)** MCP-1 **(F)** IFN-γ **(G)** TNF-α **(H)** IL-10. **(I)** BALF levels of IL-1β at 0 (WT n=3, SPC^{cre}/HOIL-1L$^{fl/fl}$ n=4) and 5 (n=10) d.p.i. **(J)** *Il1b* mRNA expression in AT2 cells at 0 (n=3) and 5 (n=4) d.p.i. **(K)** Representative Immunoblot of Caspase-1 cleavage in AT2 cells at 0 and 5 d.p.i.(n=2). **(L-N)** Immune populations were

analyzed in whole lung homogenate by FACS at 0 (n=7) and 3, 5, 7 d.p.i. (n=10). **(G)** SiglecF^{hi}CD11c^{hi} Alveolar Macrophages **(H)** Ly6G^{+}CD11b^{+}CD24^{+} Neutrophils **(I)** CD44^{+}CD62L^{-}CD4^{+} T cells. Mean ± s.d overlaid with individual data points representing replicates are depicted, *P < 0.05, **P < 0.01, ***P < 0.005, ****P < 0.0001 (one-way ANOVA followed by Bonferroni post-hoc test).

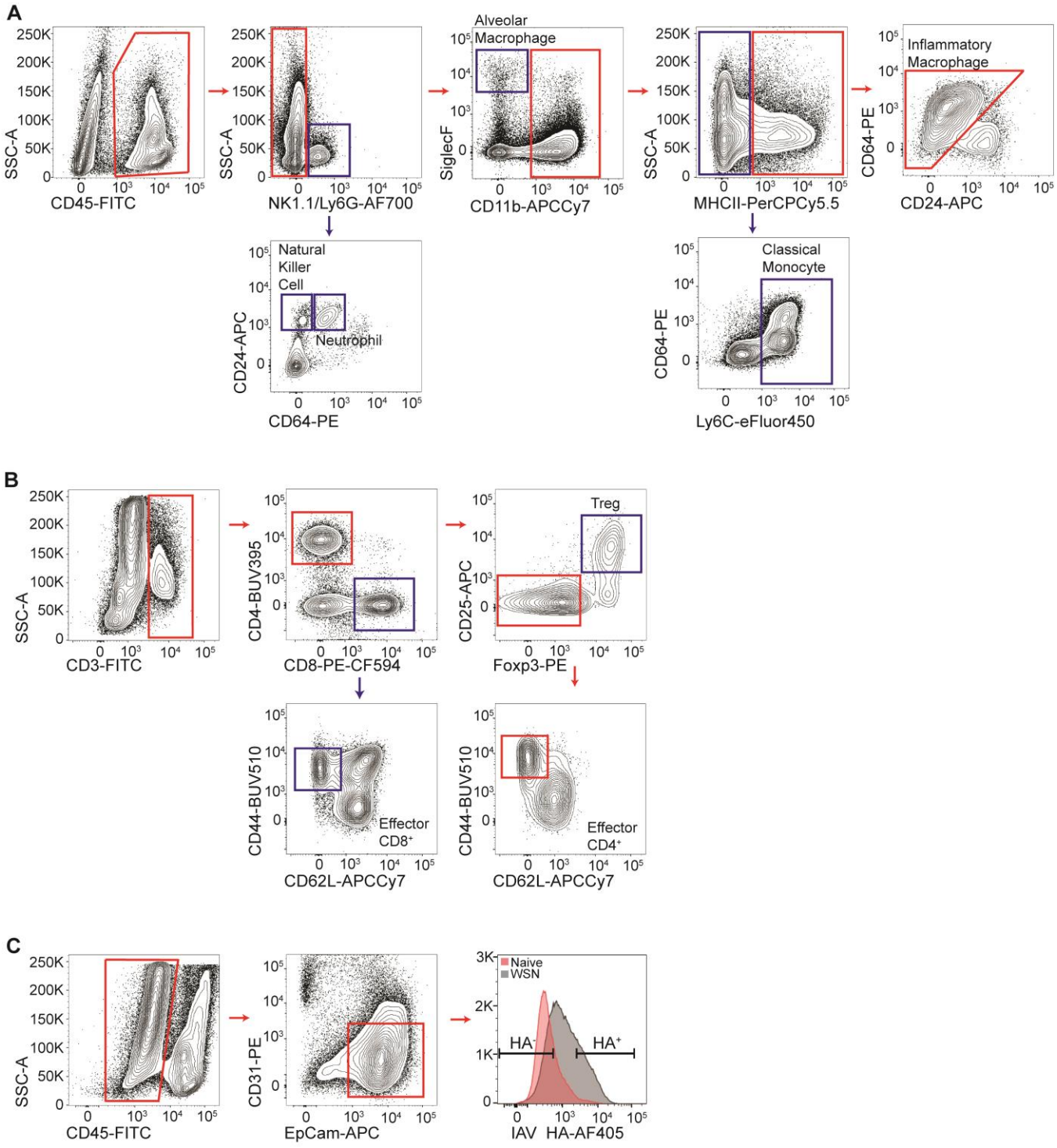

Supplemental Figure 3. Flow cytometric gating strategies.

Representative panel for identification of **(a)** myeloid cell populations using known lineage markers, **(b)** lymphoid cell populations using known lineage markers, **(c)** AT2 cells using known surface markers with the addition of influenza virus surface protein HA for separation of infected (HA^+) and non-infected (HA^-) cells.

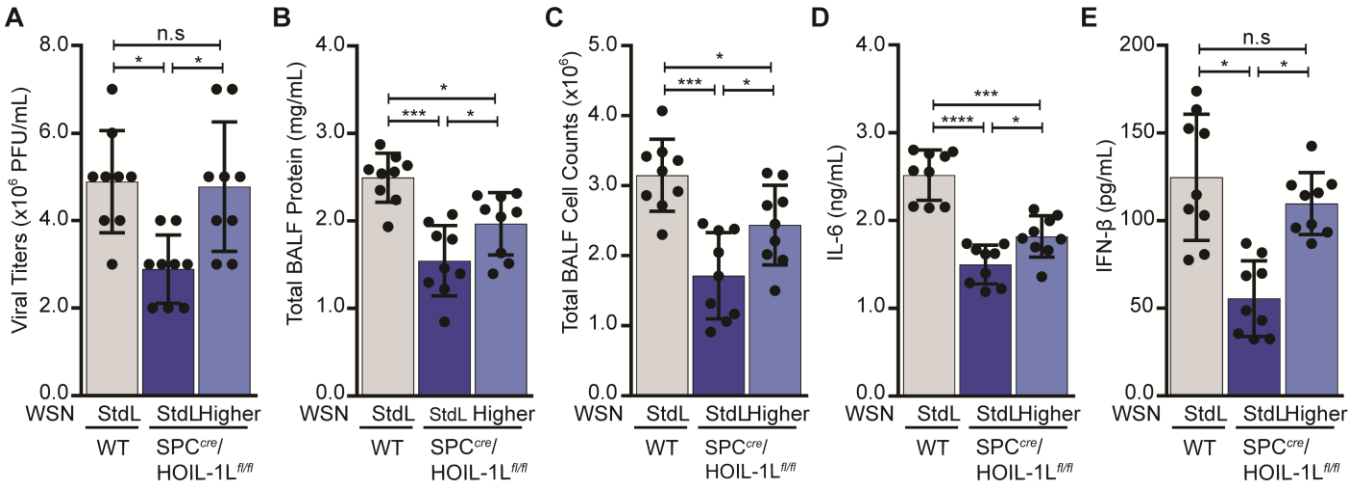

Supplemental Figure 4. SPC^{cre}/HOIL-1L$^{fl/fl}$ mice challenged with higher doses of IAV remain protected.

WT and SPC^{cre}/HOIL-1L$^{fl/fl}$ mice were i.t. infected with a standard lethal dose (StdL) of WSN, a group of SPC^{cre}/HOIL-1L$^{fl/fl}$ mice receiving a 30% higher dose (Higher). **(A)** Viral load as measured by plaque assay in whole lung BALF was collected for analysis of **(B)** total protein, **(C)** total cell count, **(D)** IL-6 **(E)** IFN-β. A-E (n=9) Mean ± s.d. overlaid with individual data points representing replicates are depicted, *P < 0.05, **P < 0.01, ***P < 0.005, ****P < 0.0001 (one-way ANOVA followed by Bonferroni post-hoc test).

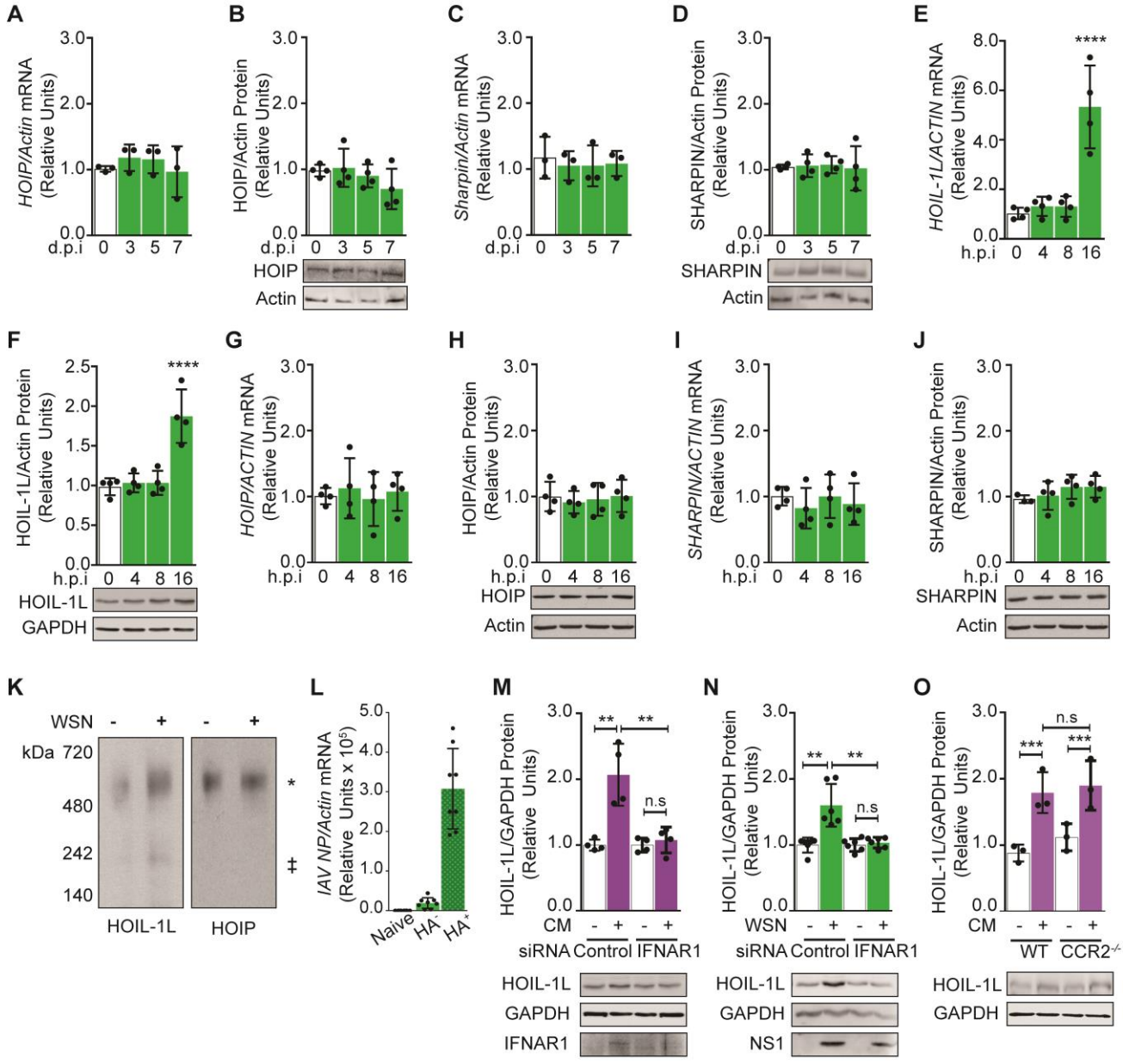

Supplemental Figure 5. HOIL-1L is upregulated during IAV infection though the type I interferon receptor signaling axis. (A-D) AT2 cells were isolated from WT mice 0, 3, 5 and 7 d.p.i. **(A,C)** mRNA levels and **(B,D)** representative immunoblots and quantifications depicted. **(A)** HOIP mRNA (n=3) **(B)** HOIP protein expression (n=4). **(C)** SHARPIN mRNA (n=4) **(D)** SHARPIN protein expression (n=4). **(E-J)** A549 cells infected for 0, 4, 8 and 16 hours with WSN. **(E,G,I)** mRNA levels and (**F,H,J**) representative immunoblots and quantifications depicted. **(E)** HOIL-1L mRNA (n=4) **(F)** HOIL-1L protein expression (n=5). **(G)** HOIP mRNA (n=3) **(H)** HOIP protein expression (n=4). **(I)** SHARPIN mRNA (n=3) **(J)** SHARPIN protein expression (n=4). **(K)** Representative Native PAGE immunoblot of LUBAC formation in A549 cells treated with WSN (n=3) **(L)** NP mRNA expression in AT2 sorted based on expression of viral HA (n=9). **(M-N)** Representative Immunoblot and

quantification of HOIL-1L expression in A549 cells transfected with siControl or siIFNAR1 and treated with **(M)** CM (n=4) **(N)** WSN (n=4) **(O)** Representative Immunoblot and quantification of HOIL-1L expression in WT and CCR2$^{-/-}$ AEC treated with CM in vitro (n=3). Blots in **H,J** from same blot with loading control shown twice. Means ±SD overlaid with Individual data points representing replicates are depicted, *P < 0.05, **P < 0.01, ***P < 0.005, ****P < 0.0001 (one-way ANOVA followed by Bonferroni post-hoc test).

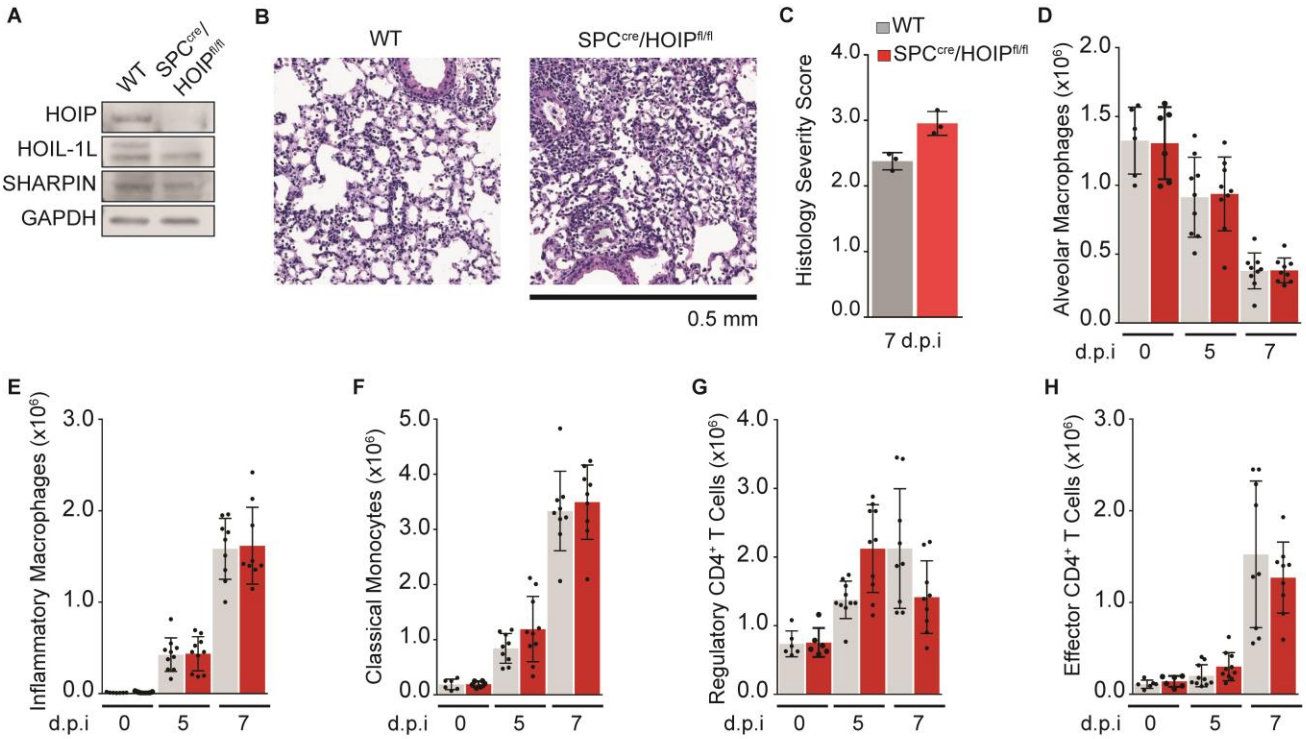

Supplemental Figure 6. Effect of loss of alveolar epithelial HOIP on host inflammatory response to IAV.

(A) Representative immunoblot showing HOIP, HOIL-1L and SHARPIN expression in isolated mouse AT2 from WT and SPC^{cre}/HOIP$^{fl/fl}$ mice. **(B)** Brightfield images of lung sections from WT and SPC^{cre}/HOILP$^{fl/fl}$ mice at 7 d.p.i stained with H&E, and **(C)** quantified for severity of lung injury as defined in Methods (Scale bar, 0.5 mm.) **(D-H)** Whole lung immune cell populations at 0, 3, 5 and 7 (n=9) d.p.i were analyzed by flow cytometry. **(D)** SiglecF^{hi}CD11c^{hi} Alveolar Macrophages **(E)** CD11b^{hi}MHCII^{hi}CD24^{low}CD64^{hi} inflammatory macrophages **(F)** CD11b^{hi}MHCII^{low}Ly6C^{hi} monocytes **(G)** CD4^{+}CD25^{+}Foxp3^{+} T_{reg} cells **(H)** CD44^{+}CD62L^{-}CD4^{+} T cells. Means ±SD overlaid with individual data points representing replicates are depicted, **P* < 0.05, ***P* < 0.01, ****P* < 0.005, *****P* < 0.0001 (one-way ANOVA followed by Bonferroni post-hoc test).

A

SNP	Ensembl Transcript ID	Position in transcript	Codon Change	Position in protein	Amino acid Change	SIFT (Sorting Intolerant From Tolerant)	PolyPhen (Polymor-phism Phenotyping)
rs2277484	ENST00000324103	3501 (out of 3627)	GTA/TTA	1061 (out of 1072)	Val/Ile	Deleterious (0.01)	Possibly damaging (0.573)

B

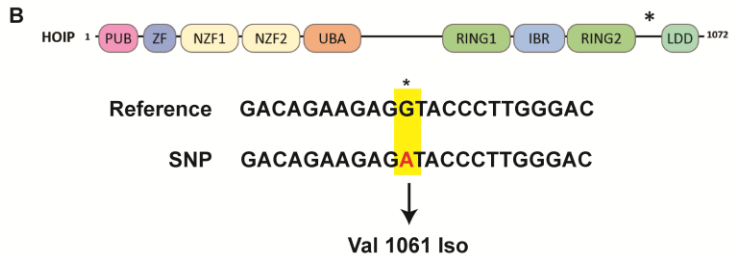

Supplemental Figure 7. HOIP SNP in AA cohort may affect "catalytic core". (A) The consequence of rs2277484 on HOIP (RNF31) transcript is deleterious and possibly damaging based on SIFT and PolyPhen. **(B)** Schematic of HOIP domains depicting location of amino acid change (Val1061Iso).

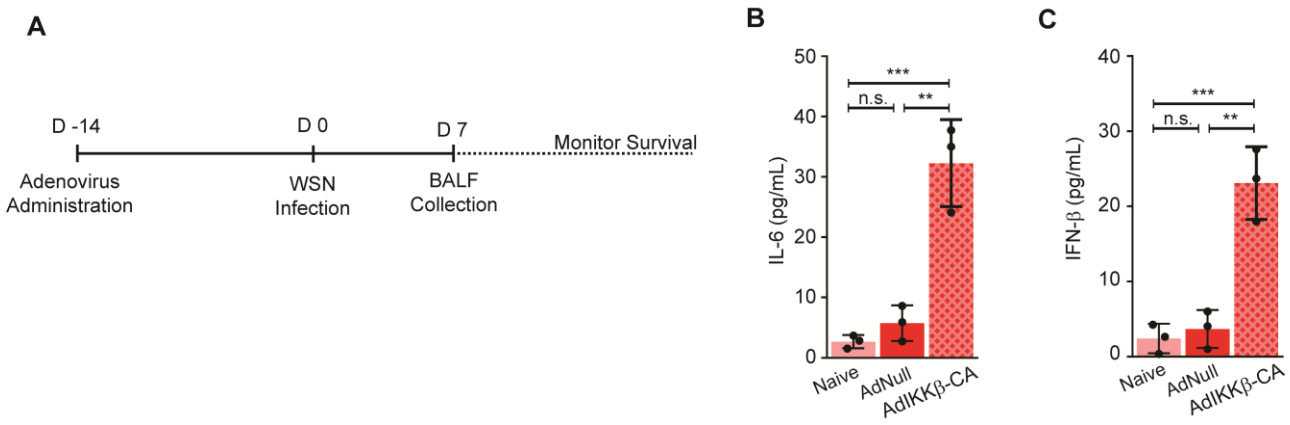

Supplemental Figure 8. Rescue of NF-κB signaling in SPC^{cre}/HOIP$^{fl/fl}$ mice with AdIKK-β-CA triggers antiviral response (A) Timeline of adenovirus administration prior to WSN infection. **(B-C)** BALF from SPC^{cre}/HOIP$^{fl/fl}$ mice naïve or administered either AdNull or AdIKK-β-CA was collected (n=3) and analyzed for **(B)** IL-6 and **(C)** IFN-β levels. Mean ± s.d overlaid with Individual data points representing replicates are depicted, **P* < 0.05, ***P* < 0.01, ****P* < 0.005, *****P* < 0.0001. (**B**, one-way ANOVA followed by Bonferroni post-hoc test).

Supplemental Table 1: Immunoblot Primary Antibodies

Target	Clone	Source	Cat. No.	Concentration	Lot
IFNAR1	MAR1-5A3	Biolegend	127301	1:1000	B163671
HOIL-1L (C-term)	2E2	Millipore	MABC576	1:1000	2915256
HOIL-1L(N-term)	N/A	K. Iwai (33)	N/A	1:1000	N/A
HOIP	N/A	Abcam	ab46322	1:1000	GR3176796-2
SHARPIN	N/A	Cell Signaling	4444S	1:1000	1
GAPDH	D16H11	Cell Signaling	2118	1:1000	6
Actin	N/A	Sigma	A2066	1:1000	018M4753V
phospo-IkBa	5A5	Cell Signaling	9246	1:1000	19
total-IkBa	L35A5	Cell Signaling	4814	1:1000	17
phospo-IRF3	4D4G	Cell Signaling	4947	1:1000	3
total-IRF3	EP2419Y	Millipore	MABf20	1:1000	NRG1817797
IRF1	13H3A44	Biolegend	657602	1:1000	B174685
RIG-I	Alme-1	Enzo	ALX-804-960	1:1000	6281213
NS1	N/A	Thermo Fisher	PA5-32243	1:1000	RH2247201
NEMO	DA10-12	Cell Signaling	2695	1:1000	3
Linear Ubiquitin	LUB9	Life Sensors	AB130	1:1000	1
IKKbeta	W15160A	Biolegend	688402	1:1000	B220786
NEMO (IP)	FL-419	Santa Cruz	sc-8330	1/50	B0615
IRF1 (ChIP)	c-20	Santa Cruz	sc-497	10ug	C1913

Supplemental Table 2: Antibodies for Myeloid Flow Cytometry

Target	Fluorophore	Clone	Source	Cat. No.	Concentration	Lot
CD45	FITC	30-F11	eBioscience	11-0451-81	2 µg/mL	4277449
MHCII	PerCP/Cy5.5	M5/114.152	Biolegend	107626	0.6 µg/mL	B209411
Ly6C	AmyCyan (eFluor450)	hk1.4	eBioscience	48-5932-80	0.4 µg/mL	4306742
LY6G	Alexa700	1A8	BD Bioscience	561236	2 µg/mL	6102838
NK1.1	Alexa700	PK136	BD Bioscience	560515	2 µg/mL	6137598
CD11b	APC-Cy7	M1/70	Biolegend	101225	0.4 µg/mL	B213160
CD11c	PE-Cy7	HL3	BD Bioscience	561022	0.4 µg/mL	6033690
CD24	APC	M1/69	eBioscience	17-0242-80	0.6 µg/mL	E14923-105
SiglecF	PE-CF594	E50-2440	BD Bioscience	562757	0.4 µg/mL	7292939
Viability	eFluor506	N/A	Invitrogen	65-0866-14	1:1000	1923275

Supplemental Table 3: Antibodies for Lymphoid Flow Cytometry

Target	Fluorophore	Clone	Source	Cat. No.	Concentration	Lot
CD3e	FITC	145-2C11	Invitrogen	11-0031-81	2 µg/mL	4323281
CD8	PE-CF594 / TexRed	53-6.7	Biolegend	100762	1 µg/mL	B200503
CD25	APC	PC61.5	eBioscience	17-0251-82	2 µg/mL	4276862
CD62L	APCe780	MEL-14	eBioscience	47-0621-82	1 µg/mL	4272740
CD44	BV510	IM7	Biolegend	103043	1.5 µg/mL	B240582
CD4	BUV395	GK1.5	BD Bioscience	563790	2 µg/mL	6336811
Foxp3	PE	FJK-16s	eBioscience	15-5773-82	4 µg/mL	4323635
Viability	UV	N/A	invitrogen	L34961	1:1000	1724751

Supplemental Table 4: Antibodies for AT2 Flow Cytometry

Target	Fluorophore	Clone	Source	Cat. No.	Concentration	Lot
EpCAM	APC	G8.8	eBioscience	17-5791-80	0.40 µg/mL	4289559
CD45	FITC	30-F11	eBioscience	11-0451-81	2.00 µg/mL	4277449
CD31	PE	390	Invitrogen	12-0311-81	0.40 µg/mL	E01191
IAV HA	AF405	IVC102	Novus	NB100-65047AF405	7.00 µg/mL	210515-091217-AF405
Viability	eFluor506	N/A	Invitrogen	65-0866-14	1:1000	1923275

Supplemental Table 5: qRT-PCR Primer Pairs

Target	Species	Forward	Reverse
Actin	Mouse	5’-GGCTGTATTCCCCTCCATCG-3’	5-CCAGTTGGTAACAATGCCATGT-3’
HOIL-1L	Mouse	5’-GATGTCAACGAGTTCACCTG-3’	5’-TCCTTCTTCTGCACCACA-3’
HOIP	Mouse	5’-GGTCTTCTCAGCTCTCCA-3’	5’-CACACTCCTCTACAGCTTCA-3’
Sharpin	Mouse	5’-ATGCCTGAACGAAGCCTT-3’	5’-TTGGGAGACTGGAACTGG-3’
IL-6	Mouse	5’-TAGTCCTTCCTACCCCAATTTCC-3’	5’-TTGGTCCTTAGCCACTCCTTC-3’
MCP-1	Mouse	5’-TTAAAAACCTGGATCGGAACCAA-3’	5’-GCATTAGCTTCAGATTTACGGGT-3’
IFN-β	Mouse	5’-CAGCTCCAAGAAAGGACGAAC-3’	5’-GGCAGTGTAACTCTTCTGCAT-3’
Actin	Human	5’-CTGGACTTCGAGCAAGAGATGG-3’	5’-AGGAAGGAAGGCTGGAAGAGTG-3’
HOIL-1L	Human	5’-CTTCATTGACAACACCTACTC-3’	5’-TGAACTCATTGACATCATCCT-3’
HOIP	Human	5’-TTTACGCCAAGAATAAATGTCC-3’	5’-CTCCTTCTGCTCTATCACTC-3’
Sharpin	Human	5’-GACCTAGCCCTCAGCA-3’	5’-CTACACATCTCACAGCCA-3’
NP	IAV	5’-CTCGTCGCTTATGACAAAGAAG-3’	5’-AGATCATCATGTGAGTCAGAC-3’